Phasic locus coeruleus activity regulates cortical encoding of salience information

Elena M. Vazey[a,1], David E. Moorman[b], and Gary Aston-Jones[c,1]

[a]Department of Biology, University of Massachusetts, Amherst, MA 01003; [b]Department of Psychological and Brain Sciences, University of Massachusetts, Amherst, MA 01003; and [c]Brain Health Institute, Rutgers University, Piscataway, NJ 08854

Edited by Ranulfo Romo, Universidad Nacional Autonóma de México, Mexico City, D.F., Mexico, and approved August 16, 2018 (received for review March 2, 2018)

Phasic activation of locus coeruleus (LC)-norepinephrine (NE) neurons is associated with focused attention and behavioral responses to salient stimuli. We used cell-type–specific optogenetics and single-unit neurophysiology to identify how LC activity influences neural encoding of sensory information. We found that phasic, but not tonic, LC-NE photoactivation generated a distinct event-related potential (ERP) across cortical regions. Salient sensory stimuli (which innately trigger phasic LC activity) produced strong excitatory cortical responses during this ERP window. Application of weaker, nonsalient stimuli produced limited responses, but these responses were elevated to salient stimulus levels when they were temporally locked with phasic LC photoactivation. These results demonstrate that phasic LC activity enhances cortical encoding of salient stimuli by facilitating long-latency signals within target regions in response to stimulus intensity/salience. The LC-driven salience signal identified here provides a measure of phasic LC activity that can be used to investigate the LC's role in attentional processing across species.

somatosensory cortex | norepinephrine | phasic | intensity coding | ERP

The noradrenergic nucleus locus coeruleus (LC) projects throughout the central nervous system and is the near-exclusive source of norepinephrine (NE) in cortical areas. The LC sends strong projections to primary sensory regions (1, 2) and has long been posited to have an important role in modulating sensory encoding. LC neurons fire in two distinct modes: tonic, characterized by irregular but continuous baseline activity (one to six spikes per second), and phasic, during which cells fire short (<300 ms) bursts of higher frequency activity (10–15 spikes per second), which can occur spontaneously but are also associated with salient stimuli and decisions (3–5). LC activity switches between these modes across behavioral states (as reviewed in refs. 5–7). Predominantly high tonic LC activity occurs with exploratory behavior and high distractibility associated with decreased task utility or stress (5). In contrast, phasic LC activity occurs during focused task performance and high utility, when levels of tonic LC activity are moderate. Phasic LC activity can be internally triggered by decision completion when a subject is performing a cognitive task, facilitating adaptive behavioral responses (3). Phasic LC can also be externally triggered by unexpected, intense, or otherwise salient stimuli that drive context-appropriate adaptive behavioral responses (e.g., alerting, orienting) (4, 8). Internally or externally generated phasic LC activity is thought to facilitate behavioral responses by increasing gain in target neurons at precise, task-relevant times, thus driving target circuits toward action thresholds. However, questions remain regarding the dynamics of LC-NE regulation of cortical attention and sensory processing. To address these, we investigated how LC firing modes impact cortical processing of external stimuli, so as to clarify the causal relationship between LC and cortical gain.

LC-NE influence over cortical sensory processing has been widely investigated. Ionotophoretically applied NE suppresses spontaneous activity and increases sensitivity of cortical neurons to subthreshold inputs, although some studies have reported signal enhancement with no change in baseline activity (9–11). Reductions in sensory thresholds or increases in evoked responsiveness after exogenous NE occur across multiple sensory modalities (10, 12–14). Electrical activation of brainstem sites in and around LC before sensory events can modulate a range of sensory-evoked responses, but results have not been consistent (15–18). There is a consistent temporal relationship between task-relevant sensory events and sensory-evoked phasic LC activity, the consequences of which have not been thoroughly investigated. Salient somatosensory or auditory stimuli trigger rapid phasic LC responses with an ∼20-ms offset, whereas salient visual cues trigger phasic LC responses ∼50–60 ms after the stimulus (4, 19–21). Exogenous NE application or electrical LC stimulation has limited ability to recapitulate this temporally precise response specifically in LC-NE neurons. Direct NE application loses specific temporal and synaptic dynamics of innate phasic LC activity. Electrical stimulation is unable to ensure cell-type specificity, can generate recording artifacts that occlude responses, and is frequently employed with extended high-frequency "phasic" stimulation trains that do not reflect normal phasic activity in vivo. Some studies have used naturalistic phasic stimulation patterns to investigate LC impact on sensory processing (18), but none have reproduced the temporal dynamics of stimulus-evoked phasic LC activity.

Significance

Locus coeruleus (LC) function has been associated with focused attention across species. LC neurons fire tonically or with short phasic bursts. We found that phasic, but not tonic, LC activity produced attentional signals across cortex, including the P300 event-related potential, and revealed distinct long-latency signals in sensory networks. These long-latency signals were seen in subpopulations normally activated by intense or salient stimuli, meaning that phasic LC activation produced salience in sensory neurons. Phasic LC-generated sensory salience signals were tightly temporally regulated, and precisely timed phasic LC activation was able to generate "false salience" in sensory processing networks, in the absence of intense stimuli. Importantly, LC-induced salience signals occurred without changes in arousal, demonstrating independent mechanisms of LC-mediated arousal and attention.

Author contributions: E.M.V. and G.A.-J. designed research; E.M.V. and D.E.M. performed research; E.M.V. and D.E.M. analyzed data; and E.M.V., D.E.M., and G.A.-J. wrote the paper.

The authors declare no conflict of interest.

This article is a PNAS Direct Submission.

[1]To whom correspondence may be addressed. Email: evazey@umass.edu or aston.jones@rutgers.edu.

This article contains supporting information online at www.pnas.org/lookup/suppl/doi:10.1073/pnas.1803716115/-/DCSupplemental.

Published online September 19, 2018.

To clarify the relationship between LC activity and modulation of cortical encoding of sensory information, we characterized the impact of sensory-locked phasic LC activation on global cortical potentials and local activity within the primary somatosensory cortex (S1) of anesthetized rats. We compared cortical changes driven by sensory-locked phasic LC activation with changes driven by tonic LC activation using optogenetics to recapitulate the innate temporal relationship between somatosensory stimuli and LC activity. We show that selective LC activation shortly following somatosensory stimuli potentiates evoked cortical neuronal responses, and recruits a unique population of "LC-gated" cortical neurons to sensory encoding. We further demonstrate that phasic LC-NE photoactivation generates a cortical event-related potential (ERP) that includes N100- and P300-like components, features often used in human ERP studies to indicate stimulus-evoked attention. Using activation patterns that mimic observed LC discharges in vivo, we were able to elicit these changes without altering global arousal. Our data reveal that LC activation modulates cortical encoding of stimulus intensity-like features in a temporally specific manner, and provides a mechanism by which phasic LC activity mediates adaptive gain in cortical targets engaged in context-appropriate neural processing. These results demonstrate a particular role for phasic LC-NE bursts in attentional regulation, separable from the role of LC in arousal, via their influences on both sensory cortical neuronal processing as well as global cortical ERP activation. Thus, in addition to providing insight into LC-NE regulation of cortical circuit function, these findings are relevant for our understanding of the neuromodulatory control of ERP signatures of attention, which are findings of interest in both animal and human cognitive research.

Results

Phasic Optogenetic Stimulation Mimics LC-NE Neuron Responses Observed After Salient Stimuli. To establish physiologically relevant, cell-type–specific control of LC-NE neurons in vivo, we expressed channelrhodopsin-2 (ChR2) or mCherry control constructs in LC-NE neurons of outbred Long–Evans rats using the synthetic promoter PRSx8 (22–24). Electrophysiologically guided vector delivery led to stable, robust expression restricted within LC-NE and subcoerulear NE neurons (Fig. 1 *A*–*C*). We quantified the specificity of LC-NE expression in a subset of subjects after physiological recording studies. We confirmed that PRSx8-driven transgene expression was highly restricted to tyrosine hydroxylase-positive NE neurons within the LC region (ChR2: 98 ± 1.0%, mCherry: 98 ± 0.6%; total: $n = 7$ animals, $n =$ 10 vector injections, $n = 1{,}430$ neurons).

We used single-unit in vivo electrophysiology in isoflurane-anesthetized rats to validate our ability to drive activity of LC-NE neurons within the physiological range (Fig. 1*D*). LC neurons in rats with PRSx8-ChR2 vector injections ($n = 22$ cells, $n = 8$ animals) responded to pulses (10–20 ms) of 473-nm light with short-latency single-action potentials that could be entrained tonically (single 10-ms pulses, 0.5–10 Hz; Fig. 1*E*) or with phasic bursts of light pulses (three to four pulses at 12 Hz; Fig. 1*F*). We found that phasic photoactivation of LC neurons was followed by a transient inhibition, similar to LC activity evoked by sensory stimuli. The median evoked response magnitude [RMag = (evoked count post stimulus − baseline activity)/number of trials] for phasic LC photoactivation was 0.50, and the average inhibition duration after phasic photoactivation was 982 ± 200 ms. These values were not different from those evoked by high-intensity (10 mA) hind-paw stimulation (laser vs. hind-paw stimulation: $P = 0.474$, Mann–Whitney U test; $n = 15$ cells). These results confirm that PRSx8-ChR2 in LC-NE neurons can be used to drive tonic and phasic photoactivation across physiologically relevant frequencies and that photoactivation responses faithfully reproduce innate activity patterns.

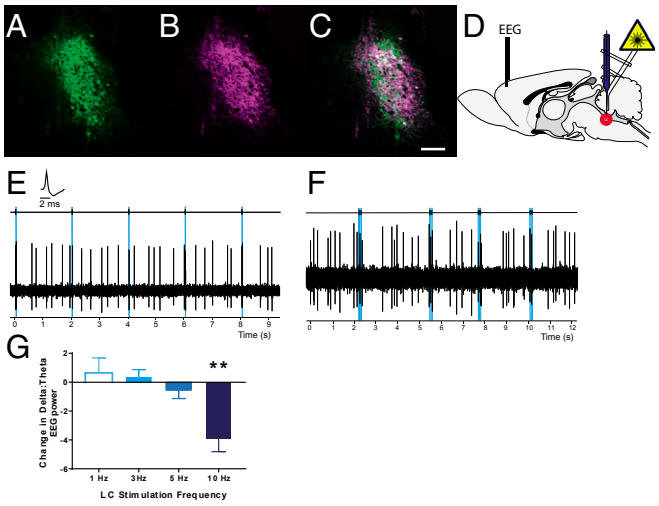

Fig. 1. Selective optogenetic control of LC-NE neurons at subarousal levels. LC neurons identified with TH staining (*A*, green) were transduced to selectively express ChR2-mCherry (*B*, magenta) at high levels (*C*, merge). (Scale bar: 100 μm.) (*D*) Schematic of glass pipette optrode and PFC EEG recording configurations. (*E*) Pulses of blue light elicited reliable short-latency single-action potentials from LC neurons in vivo (*Inset*, LC unit waveform) at 1 Hz up to 15 Hz. (*F*) Short trains of 15-Hz phasic light pulses evoked phasic excitation of LC neurons, followed by a postactivation inhibition pattern comparable to innate phasic LC responses to salient stimuli. (*G*) Increases in tonic LC stimulation dose-dependently increased arousal, as seen by a reduction in δ-dominant EEG recordings at frequencies >5 Hz. $^{**}P < 0.01$ relative to baseline arousal.

Optogenetic LC Activation Frequency Defines Cortical Arousal Threshold. Manipulation of LC-NE function can globally change cortical state (25). Changes in EEG indices of arousal have been demonstrated after sustained or high-frequency optogenetic or chemogenetic activation of LC-NE neurons even under isoflurane anesthesia (23, 26). We sought to determine whether all physiological LC manipulations fundamentally alter cortical arousal. We measured changes in the ratio of δ to θ EEG power during LC activation relative to baseline before photoactivation. In concordance with previous studies, optogenetic activation of LC-NE neurons at 5 Hz or more increased cortical measures of arousal by decreasing δ dominance in the EEG (Fig. 1*G*). Increases in cortical arousal during tonic LC photoactivation were dependent upon the frequency of LC stimulation ($P = 0.002$, one-way ANOVA; $n = 5$–6 animals per frequency). Low-frequency LC activation (<5 Hz) did not change arousal under anesthesia, identifying a threshold within which to probe LC influence on cortical function without global changes in cortical state.

Phasic, Not Tonic, LC Activation Evokes Cortical P300-Like ERP Responses. Using photoactivation parameters that do not alter EEG indices as used above, we compared changes in cortical signaling triggered by different patterns of LC activity: either tonic (3 Hz) or bursts of phasic LC activity (12 Hz, three pulses, 0.5 burst per second) in anesthetized rats (Fig. 2 *A* and *B*). These LC activity patterns are similar to those reported from LC neurons during distractibility or mild stress (tonic) or after presentation of salient sensory stimuli (phasic) in awake or anesthetized animals (3, 4, 27). This sought to determine whether these LC activity patterns can generate a global cortical response distinct from driving arousal.

As expected, based on the arousal threshold identified above, these phasic and tonic LC patterns did not change cortical arousal during stimulation sustained throughout 100-s epochs [one-way repeated measures (RM) ANOVA: $F_{(1.744,\ 19.17)} = 0.5439$, $P = 0.57$; Fig. 2*C*]. We examined ERPs from surface-to-depth electrodes in

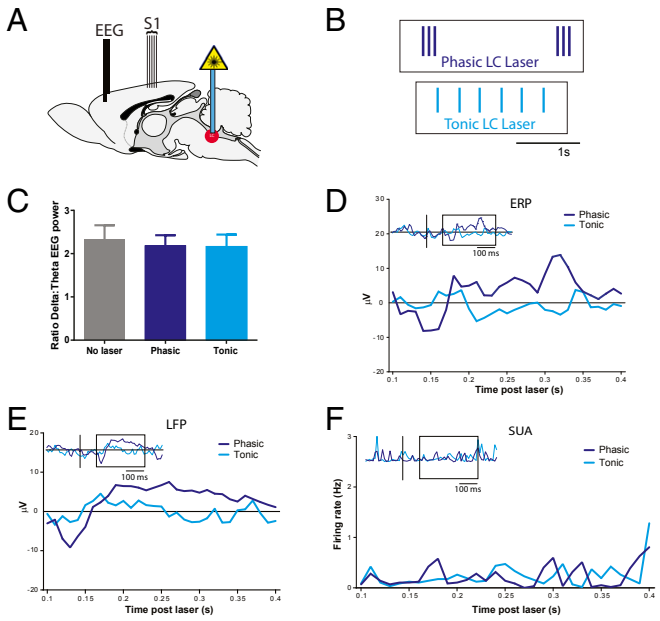

Fig. 2. Phasic LC drives responses across cortical target regions. (*A*) Schematic showing location of prefrontal EEG electrodes for recording ERPs and S1 electrodes for recording LFPs during blocks of tonic or phasic optogenetic LC stimulation. (*B*) Excerpts of laser pulse trains used for LC photoactivation: tonic (3-Hz continuous, cyan blue) or phasic (three-pulse 12 Hz every 0.5 Hz, dark blue). (Scale bar: 1 s.) (*C*) Graph showing no change in δ dominance of EEG recording over 100 s for either phasic or tonic LC photoactivation. (*D*) Average PFC ERP signal across 100 s of continuous LC photoactivation ($n = 16$ recordings, $n = 6$ animals, 50 trials, 2 s per trial) from 100 to 400 ms after laser pulse onset (expansion of boxed region in *Inset*). (*Inset*) Extended cortical ERP at −0.2 s through +0.5 s post-LC stimulation with line at laser onset. Phasic-LC ERPs (dark blue lines) show both N100-like (130-ms latency) and P300-like (330-ms latency) components. (*E*) Averaged LFP signal from S1 cortex from 100 to 400 ms after laser pulse onset during 100 s of continuous LC photoactivation showing N100-like and P300-like responses after phasic (dark blue lines) LC bursting ($n = 18$ recordings, $n = 7$ animals) (*Inset*, extended LFP at −0.2 s through +0.5 s post-LC stimulation with line at laser onset). (*F*) Neither tonic (cyan blue) nor phasic (dark blue) LC activation alone caused temporally specific changes in S1 single-unit activity (SUA; $n = 135$ units, 18 recordings from seven animals) (*Inset*) S1 SUA at −0.2 through +0.5 s with line at laser onset.

medial prefrontal cortex (mPFC) to determine if tonic or phasic LC activation could modulate cortical networks in the absence of changes in overall arousal. Phasic, but not tonic, LC photoactivation generated a distinct cortical ERP in mPFC (Fig. 2*D*). When averaged across 50 trials (2-s interval), phasic LC-evoked ERPs had a negative peak at ∼130 ms after laser onset, similar to the N100 associated with sensory detection, and a second positive peak at ∼330 ms, in line with the time window for a P300-like ERP, typically elicited upon recognition of salient stimuli (28, 29). In contrast, despite twice the number of pulses per unit time, tonic 3-Hz LC activation did not change mPFC EEG signals when averaged across 50 activation trials (2-s interval, inclusive of six pulses) locked to the beginning of tonic firing (to parallel averaging for phasic analysis) or when averaged across 300 trials locked to each tonic laser pulse (sliding window analysis). The generation of ERPs similar to N100 and P300 after phasic, but not tonic, LC activation illustrates a major selective feature in cortical responses to phasic LC activity.

In addition to global modulation as measured in ERP activity, we investigated LC-driven changes in S1. This area has a well-defined physiological response to external stimuli and receives prominent LC inputs. Local field potentials (LFPs) recorded from electrode arrays in S1 (Fig. 2*E*) during LC activation showed N100- and P300-like responses to phasic, but not tonic, LC activation, similar to the phasic LC ERP in PFC described above. Surprisingly, on the same electrodes, LC-driven LFPs in S1 cortex did not trigger temporally locked action potentials in postsynaptic S1 units after tonic or phasic LC activation (Fig. 2*F*).

These data show that low levels of tonic LC activity do not elicit temporally specific changes in cortical function, whereas phasic LC bursting can produce N100- and P300-like ERPs and LFPs without driving arousal indices. Across multiple cortical regions, phasic LC activity is sufficient to generate cortical potentials similar to those associated with stimulus detection.

LC Photoactivation Reveals and Enhances Sensory-Evoked Cortical Signals. To determine how the cortical consequences of LC activity might alter sensory stimulus encoding, we applied a weak electrical stimulus (1 mA, 0.5 ms at 0.5 Hz) s.c. to the contralateral hind paw during S1 recording and LC photoactivation. Short-latency (5–50 ms) S1 excitation in response to tactile or electrical limb stimulation is well characterized in both awake and anesthetized subjects (30, 31). We recorded extracellular activity from multiple sites in deep cortical layers of S1 hind-paw regions ($n = 18$ recording sites from seven animals; Fig. 3*A*). Recorded neurons displayed canonical excitatory short-latency sensory activity, indicating sensory detection (>2 SD Z score, 10-ms bins), and these regions were densely innervated by ChR2-positive terminals from LC (Fig. 3*B*). The weak foot stimulus used to evoke sensory responses in S1 did not alter LC neuron firing (LC RMag = 0.04 ± 0.01, $n = 22$ cells). During blocks of foot stimulation (0.5 Hz), 473-nm light directed at LC was used to exogenously drive tonic (3 Hz) or phasic (2 Hz, three pulses, 0.5 bursts per second) LC activity as described above; neither of these stimulation patterns altered arousal (Fig. 3*C*). We identified 135 well-isolated S1 units present throughout all stimulation epochs [baseline (no stim), stim + no LC, stim + phasic LC, and stim + tonic LC] that also demonstrated short-latency responses (<50 ms) to paw stimulation to at least one condition either with or without LC photoactivation.

LC photoactivation significantly altered the short-latency response characteristics of S1 stimulus encoding (Fig. 3). Most S1 units ($n = 78$, 58%) were responsive to paw stimulation in the absence of LC photoactivation, eliciting a transient excitatory response. Similar to previous reports of NE-mediated effects (32), LC photoactivation enhanced these short-latency responses; we term these "LC-modulated" neurons (Fig. 3*D*). Response onset in LC-modulated neurons (median = 12–14 ms) was not altered by photoactivation [Kruskal–Wallis test, $H_{(2)} = 2.149$, $P = 0.34$]. However, the response magnitude significantly increased during photoactivation, specifically after phasic LC photoactivation [$H_{(2)} = 11.05$, $P = 0.011$]. This enhancement in short-latency responses from LC-modulated neurons developed across trials of phasic LC photoactivation.

The remaining 57 of 135 S1 neurons (42%) did not show any significant short-latency responses to the 1-mA foot stimulation in the absence of LC photoactivation. However, when blocks of hind-paw stimulation were paired with phasic or tonic LC photoactivation, these neurons demonstrated short-latency stimulus-evoked responses, with the majority of units responding under both LC activation conditions [$\chi^2_{(6)} = 81.52$, $P < 0.0001$]. We called these LC-gated neurons because their sensory response was gated by LC activation (Fig. 3*D*). Within LC-gated neurons, short-latency magnitudes did not differ between blocks of phasic vs. tonic LC photoactivation (Mann–Whitney U test tonic-gated vs. phasic-gated: $P = 0.66$). However, responses during tonic LC stimulation had a more rapid onset (11 ms) than those during phasic LC activation (16 ms; Mann–Whitney U test tonic-gated vs. phasic-gated: $P = 0.03$).

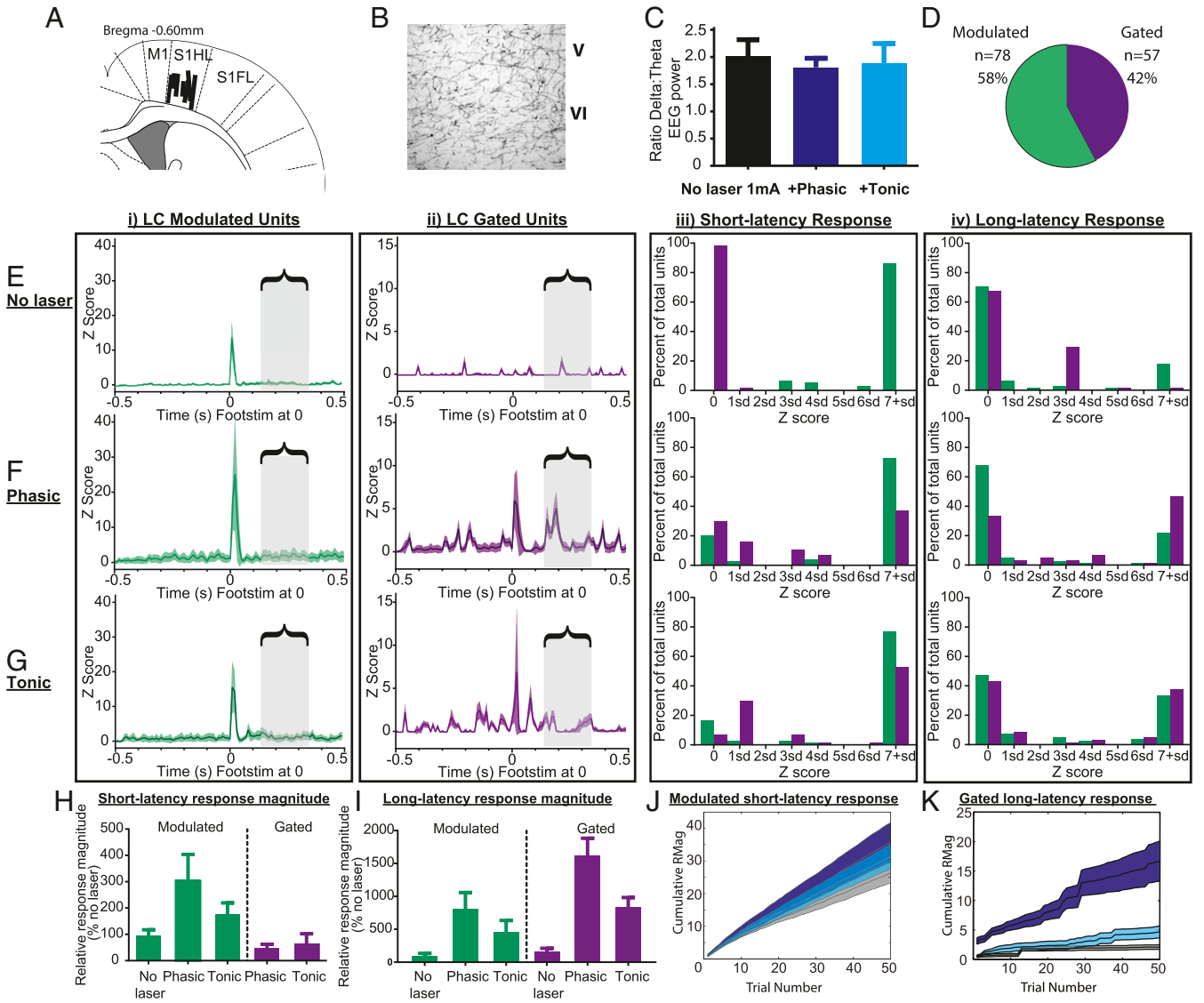

Fig. 3. LC-NE photoactivation potentiates S1-evoked responses and reveals LC-gated population. (*A*) Recordings were made from deep layers of S1 cortex; sites were at least 50 μm apart ($n = 18$ sites, $n = 7$ animals). FL, forelimb; HL, hindlimb. (*B*) Immunohistological detection of LC-ChR2 fibers and terminals within deep layers of S1 cortex. (*C*) Average δ/θ EEG ratio (a proxy for arousal) remained stable across hind-paw stimulation epochs, including during LC photoactivation. (*D*) S1 neurons were divided into two distinct populations based on their sensory responsiveness in the absence (LC-modulated neurons, green; $n = 78$ units) or presence (LC-gated neurons, purple; $n = 57$ units) of LC photoactivation. (*E*) Sensory response characteristics to low-intensity foot stimulation (Footstim) in the absence of LC photoactivation (no laser). (*i*) Response ± 95% confidence interval (CI) for LC-modulated neurons (green) averaged across 50 trials and locked to Footstim at time 0. (*ii*) Response ± 95% CI for LC-gated neurons (purple) averaged across 50 trials and locked to Footstim at time 0. (*iii*) Distributions of short-latency responses (5–50 ms), ranked by *Z* score on the *x* axis for both LC-modulated (green) and LC-gated neurons (purple), indicating the proportion of neurons participating in the short-latency response. All units significantly responded (>2 SD) within at least one condition but not necessarily in all conditions. (*iv*) Intensity distributions similar to (*iii*) showing the proportion of neurons participating in long-latency responses (130–350 ms), ranked by Z score on the *x* axis for LC-modulated (green) and LC-gated neurons (purple). The bracketed region with gray boxes throughout highlights the window within which long-latency responses were evaluated. (*F*) Sensory response characteristics to low-intensity Footstim with phasic LC photoactivation. Activity plots for LC-modulated (*i*) and LC-gated (*ii*) units during phasic photoactivation are shown as described for *E*. Intensity distributions for short-latency (*iii*) and long-latency (*iv*) response participation during phasic photoactivation blocks are shown as described in *E*. (*G*) Sensory response characteristics to low-intensity Footstim with tonic LC photoactivation. Activity plots for LC-modulated (*i*) and LC-gated (*ii*) units during phasic photoactivation are shown as described for *E*. Intensity distributions for short-latency (*iii*) and long-latency (*iv*) response participation during phasic photoactivation blocks are shown as described in *E*. (*H*) Average short-latency magnitudes, normalized as a percentage of LC-modulated neurons with no laser. (*I*) Average long-latency magnitudes, normalized as a percentage of LC-modulated neurons with no laser. (*J*) Trial-by-trial responses in LC-modulated neurons. The magnitude of short-latency responses in LC-modulated neurons accumulated steadily across trials. Phasic LC photoactivation (dark blue) potentiated responses more than tonic photoactivation (cyan blue) relative to no laser (gray). (*K*) Trial-by-trial responses for LC-gated neurons. Phasic photoactivation (dark blue) augmented the long-latency response in LC-gated neurons within individual trials and consistently accumulated across trials relative to tonic photoactivation (cyan blue) and no laser (gray).

Subsequent analysis showed that LC-gated neurons could be dissociated from LC-modulated neurons by lower basal firing properties (without LC photoactivation), indicating that they represent a distinct subpopulation within S1 ($U = 1{,}770$, $n_1 = 57$, $n_2 = 78$, $P = 0.043$). In addition to lower basal activity, LC-gated S1 neurons produced smaller short-latency evoked responses than LC-modulated neurons under each photoactivation condition [$H_{(3)} = 4.81$, $P < 0.0051$; Dunn's multiple comparison

test (MCT) tonic-gated vs. tonic-modulated: $P = 0.030$, phasic-gated vs. phasic-modulated: $P = 0.007$]. These results show that LC-NE activity elicits widespread neuronal changes in S1 sensory encoding by increasing the proportion of S1 neurons that encode sensory stimuli through the recruitment of LC-gated neurons, as well as by triggering changes in latencies and magnitudes of sensory stimulus-evoked responses.

Phasic, but Not Tonic, LC Activation Enhances Long-Latency Sensory Salience Responses in Cortex. In addition to the canonical sensory responses described above (<50-ms latency), a small number of reports noted long-latency or E2 (~100-ms+) excitations in S1 after somatosensory stimuli (30). Long-latency sensory responses can be altered by arousal states or drugs of abuse and have been hypothesized to encode subjective information about stimuli, although the driving force behind these long-latency responses remains unknown (30, 33). To better understand the role of long-latency responses in somatosensory encoding, we investigated the impact of LC activity on this window.

We identified a potent influence of phasic LC photoactivation on long-latency excitation in S1 neurons (10-ms bins: $Z > 1.96$), 130–350 ms after the sensory stimulus within our extracellular recordings (Fig. 3). Photoactivation of LC neurons increased the magnitudes of long-latency responses across conditions [$H_{(5)} = 34.02$, $P < 0.0001$; also *SI Appendix*, Table S1]. Phasic (12 Hz, three-pulse burst), but not tonic (3 Hz), LC activation increased long-latency response magnitudes in both LC-modulated and LC-gated neurons (Dunn's MCT: $P < 0.01$). During phasic LC photoactivation, the majority of long-latency responding came from LC-gated neurons and not LC-modulated neurons (Dunn's MCT: $P < 0.05$). Furthermore, enhancement of long-latency responses in LC-gated neurons occurred within a single trial of sensory-locked LC photoactivation, demonstrating that phasic LC activity can rapidly alter signaling related to a sensory stimulus (Fig. 3*K*). These results show that sensory-locked phasic LC photoactivation acutely enhances long-latency encoding of sensory information, particularly through LC-gated S1 neurons.

Phasic LC-Mediated S1 Response Enhancements Replicate Intensity Encoding. LC-NE neurons are phasically activated by both salient sensory stimuli (4) and decisions to initiate behavioral responses (3). To determine if the LC-mediated enhancement of S1 responses to low-intensity hind-paw stimulation mimics changes generated by innate stimulus intensity/salience, we compared responses in the same population of S1 neurons reported above using LC photoactivation with responses to a stronger hind-paw stimulus (3 mA, 0.5 ms) that evokes sensory-locked phasic LC activity.

LC-modulated and LC-gated S1 neurons were tested on high-intensity hind-paw stimulation without LC photoactivation. We found that the higher hind-paw stimulus intensity changed both short-latency and long-latency S1 neural responses (Fig. 4 and *SI Appendix*, Table S1). The onset of short-latency responses in LC-modulated neurons (13 ms) was shorter than in LC-gated neurons (16.5 ms) during high-intensity hind-paw stimulation; this differential latency between S1 populations was similar to that seen after low-intensity hind-paw stimulation with time-locked phasic (12 Hz, three-pulse burst) LC photoactivation [12 ms in LC-modulated vs. 16 ms in LC-gated during low-intensity phasic LC photoactivation: $H_{(5)} = 9.29$, $P = 0.037$; Dunn's MCT: $P = 0.0425$; also *SI Appendix*, Table S1]. High-intensity hind-paw stimulation also increased short-latency response magnitudes in LC-modulated neurons, again similar to phasic LC photoactivation with low-intensity sensory stimulation [RM one-way: $F_{(2.44,\ 188.2)} = 3.18$, $P = 0.034$; Holm–Sidak MCT: $P = 0.018$]. In LC-gated neurons, high-intensity hind-paw stimulation revealed short-latency response magnitudes similar to those seen with low-intensity paw stimulation accompanied by phasic or tonic LC activation [$H_{(2)} = 5.84$, $P = 0.054$]. Higher stimulus intensity also increased long-latency response magnitudes in both LC-modulated and LC-gated neurons compared with low-intensity sensory stimulation alone [$H_{(7)} = 38.61$, $P < 0.0001$]; these enhanced response magnitudes were comparable to those seen with phasic LC activation during low-intensity paw stimulation.

In sum, increases in hind-paw stimulus intensity enhanced S1 stimulus encoding in a similar manner as phasic (but not tonic) LC photoactivation. Specifically, phasic LC photoactivation potentiated short-latency responses in LC-modulated S1 neurons and recruited an LC-gated S1 population that produced large long-latency responses. Thus, intensity/salience-related changes in S1 neurons can be driven by sensory-locked phasic LC activity. These changes in S1 responses after time-locked phasic LC activation (stimulus-generated or photoactivated) enhance relevant stimulus encoding, which may assist in coordination of attention and behavioral responses across networks.

LC-Associated Salience Encoding Is Temporally Specific. In the above experiments, phasic LC photoactivation was applied 20 ms after the hind-paw stimulus to mimic the timing of innate phasic LC activation by salient stimuli (4, 34). As described above, the elevated S1 response to high-intensity paw stimulation, or to low-intensity paw stimulation with time-locked phasic LC activation, was most prominent in the long-latency component of the S1 response. This long-latency response occurred during an epoch we define as a "salience window" (130–400 ms poststimulus). During this salience window, long-latency S1 responses co-occurred with coordinated ERP and LFP responses that were all driven by phasic LC photoactivation (Fig. 4*C*).

To investigate the temporal specificity of the effects of phasic LC activity on S1 salience encoding, we shifted phasic LC photoactivation (12 Hz, three-pulse burst) so that it occurred 20 ms before the low-intensity paw stimulus and recorded extracellularly from the same population of S1 neurons. When phasic LC activation preceded the sensory stimulus in this way, the potentiation of short-latency responses in LC-modulated neurons across activation blocks remained [phasic LC before paw stimulus vs. phasic LC after paw stimulus area under the curve (AUC): $P = 0.98$]. However, the selective increase in salience-like long-latency responses for LC-gated neurons was markedly reduced (phasic pre-AUC vs. phasic post-AUC: $P < 0.0001$; Fig. 4*E*). This shows that there is a tightly regulated temporal relationship between phasic LC photoactivation and long-latency intensity/salience signaling through LC-gated neurons, where the relative timing of phasic LC activity has a strong impact on cortical responses. Phasic LC activation produces the greatest increase in cortical long-latency responses when it occurs immediately after the sensory event, similar to the temporal relationship seen with innate phasic LC responses to salient stimuli (21).

LC-Driven Intensity/Salience Encoding in S1 Is Broadly Distributed. Short-latency somatosensory responses are tuned to specific receptive fields, and subpopulations of S1 neurons respond in a topographically specific manner (31). As such, we targeted our results to 135 single units that were tuned to robustly respond to the hind paw. As described above, we found that phasic LC photoactivation augments long-latency responses in LC-gated S1 neurons in a temporally precise manner, mimicking augmented responses with higher intensity stimuli. However, long-latency responses in S1 have broader receptive fields than short-latency responses (30). The LC-NE projection network is anatomically suited to broadly drive intensity/salience encoding across multiple receptive fields. Therefore, we investigated whether phasic LC activity could drive long-latency signals in a wide population of S1 neurons that were not tuned specifically to hind-paw stimulation. For this, we took advantage of our results above showing that LC-gated neurons exhibited short-latency

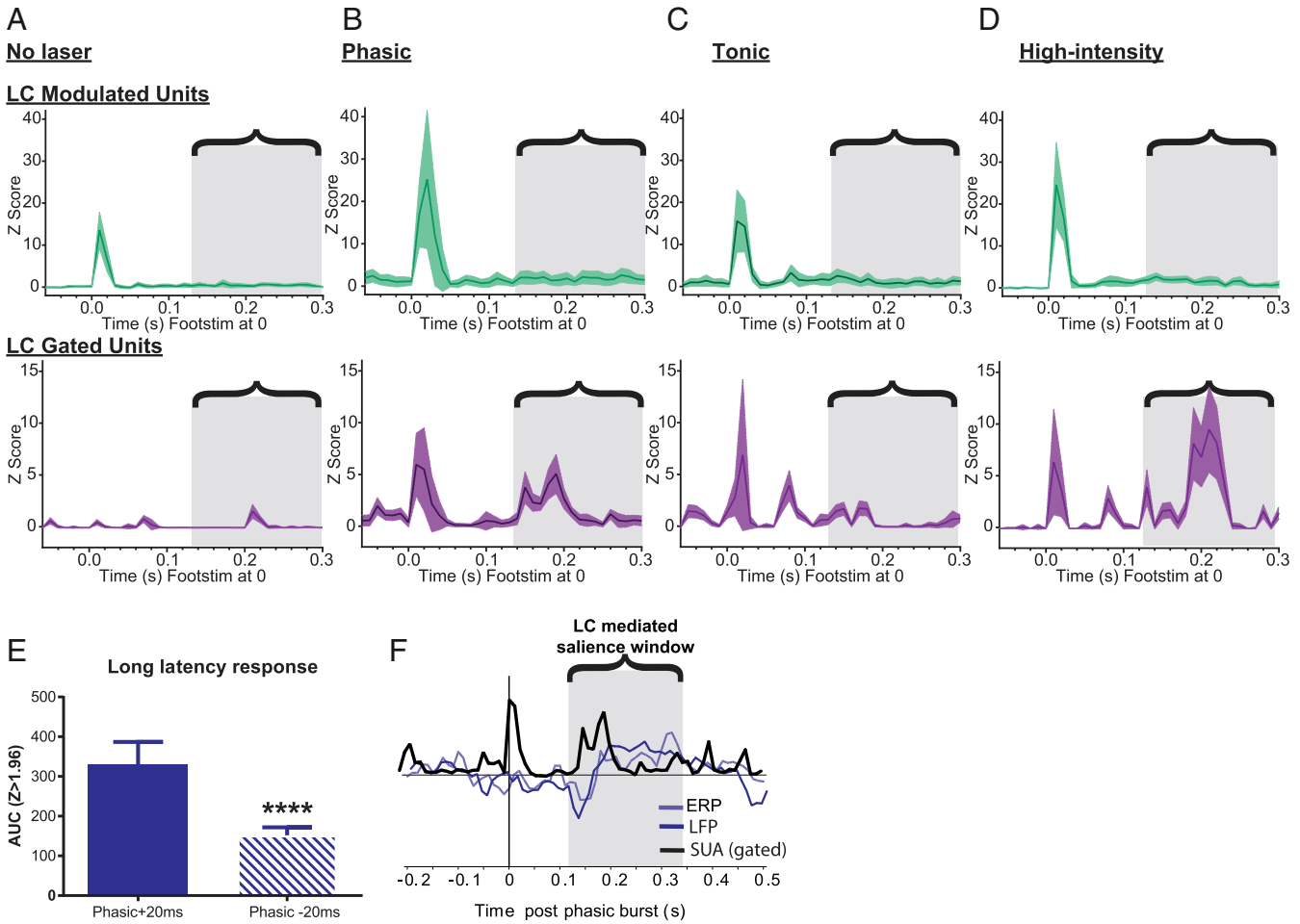

Fig. 4. Phasic, but not tonic, LC activity generates salience-like features in S1. (*A*) Response ± 95% confidence interval (CI) to low-intensity hind-paw stimulation without LC photoactivation for LC-modulated neurons (*Top*, green) and LC-gated neurons (*Bottom*, purple) averaged across 50 trials and locked to foot stimulus (Footstim) at time 0. The bracketed region with gray boxes throughout highlights the phasic LC-mediated salience window for coordinating responses across cortical targets within which long-latency responses were identified. (*B*) Response ± 95% CI to low-intensity hind-paw stimulation with time-locked phasic LC photoactivation for LC-modulated neurons (*Top*, green) and LC-gated neurons (*Bottom*, purple) averaged across 50 trials and locked to Footstim at time 0. (*C*) Response ± 95% CI to low-intensity hind-paw stimulation with time-locked tonic LC photoactivation for LC-modulated neurons (*Top*, green) and LC-gated neurons (*Bottom*, purple) averaged across 50 trials and locked to Footstim at time 0. (*D*) Response ± 95% CI to high-intensity hind-paw stimulation without LC photoactivation for LC-modulated neurons (*Top*, green) and LC-gated neurons (*Bottom*, purple) averaged across 50 trials and locked to Footstim at time 0. Note the prominent long-latency response found in *B* and *D* with phasic LC stimulation around 200 ms after the hind-paw stimulus. (*E*) Comparison of the long-latency response seen from LC-gated neurons in *B* after a temporal shift in phasic LC photoactivation from +20 ms to −20 ms before Footstim. The magnitude of the long-latency response was markedly reduced by this temporal offset. ****$P < 0.0001$. (*F*) Temporal overlay of ERP response from mPFC, LFP response from S1, and single-unit activity (SUA) response from LC-gated S1 neurons aligned to the onset of phasic LC bursting at time 0.

responses (i.e., tuning) to paw stimulation only when LC was coactivated. Using 140 additional extracellularly recorded S1 single units that did not show short-latency tuning to any stimulation either with or without LC coactivation, we looked exclusively for long-latency intensity/salience signals that appeared with paw and LC photoactivation (tonic 3-Hz or phasic 12-Hz, three-pulse burst). Within this population, we found 53 units (38%) with significant ($Z > 1.96$) long-latency responses after low-intensity paw stimulation only when LC was coactivated, a similar proportion to LC-gated neurons (42%) in hind-paw–tuned units. This result shows that phasic LC-mediated intensity/salience encoding is distributed broadly across S1 neurons (110 of 275), independent of sensory tuning.

Discussion

The Role of Phasic LC Activity in Sensory Processing. Intense or otherwise motivationally salient (e.g., conditioned) stimuli across many modalities evoke phasic LC activation (4). Many studies have investigated LC or NE modulation of cortical sensory representation, but have not reproduced the precise, innate temporal relationship between sensory stimulus and phasic LC activation. Our results show that phasic and tonic patterns of LC activity profoundly, but differentially, regulate cortical encoding of stimuli. By selectively controlling the precise timing of LC firing and sensory stimulation, we demonstrated that LC activation rapidly enhances (LC-modulated) or reveals (LC-gated) sensory-evoked responding in S1 neurons. We further identified a phasic, but not tonic, LC-driven cortical salience window (130–400 ms after paw stimulation) during which mPFC ERPs, S1 LFPs, and S1 unit responses are augmented. The augmented responses during this window were similar for low-intensity stimuli accompanied by phasic LC photoactivation and for high-intensity paw stimulation that induces innate phasic LC activation. Given that our LC stimulation profile did not cause cortical EEG arousal, our data strongly support the proposal that LC activation resulting from high-intensity stimuli contributes to

long-latency sensory responses during this temporal window to facilitate encoding of qualitative stimulus information, such as intensity/salience. We predict that these enhanced sensory responses may result from highly intense stimuli, as demonstrated here, or by conditioned or otherwise important stimuli during behavior. We propose that this LC-augmented sensory response functions to facilitate an optimal response to important stimuli, consistent with the role of phasic LC-NE bursting in regulating adaptive decision making (5, 6, 35, 36).

Phasic LC activation induced mPFC ERPs in the absence of external sensory stimuli, but did not entrain cortical unit activity. However, when time-locked to a sensory stimulus, LC-NE activation induced a saliency-like long-latency response in both an LC-modulated population and a unique population of LC-gated S1 neurons. Furthermore, this long-latency salience response was present in neurons that did not exhibit short-latency responses ("nontuned" neurons), demonstrating the broad and powerful influence of LC-NE drive on sensory processing. Thus, phasic LC photoactivation created "virtual salience" in S1 responses to weak sensory stimuli. The generation of virtual salience was exclusive to phasic LC activity, and was not induced by tonic LC activity. Long-latency responses were markedly lower when phasic LC activation preceded the paw stimulus by 20 ms (instead of the physiological latency of 20 ms after paw stimulus), confirming a temporally specific interaction between LC signaling and sensory processing. These results reveal that in awake animals, phasic LC discharges produced by salient stimuli serve as a mechanism for the engagement of sensory attention and facilitation of coordinated, likely multisensory, decision making and action planning.

LC Modulates Specific Cortical Sensory Responses. We used cell-type–specific optogenetics to drive physiological phasic and tonic patterns of LC activity and assess the impact on cortical responses in ERPs, LFPs, and single-unit activity. Our findings in LC-modulated neurons clarify mixed results from previous studies using electrical stimulation of LC or ionotophoretic application of NE in cortex (16, 18, 37, 38). In the current study, we did not see a suppression of basal activity within the subarousal tonic and phasic LC activation parameters used. This aligns with a subset of prior reports that have identified LC or NE enhancement of signal to noise in cortical responses without suppression of baseline activity with low doses of NE (11, 39–41).

The use of cell-type–specific optogenetic stimulation permitted us to uniquely modulate LC-NE in a naturalistic manner, while excluding nearby brainstem nuclei or fibers of passage. Although our manipulation was selective for LC-NE neurons, it should be noted that the downstream effects were not restricted to S1 or somatosensory pathways. In manipulating LC-NE neurons, rather than LC terminals within S1, we triggered multilevel modulation across LC projection targets, including multiple points within the somatosensory pathway, such as brainstem, thalamic relays, and directly within S1. By using physiologically relevant activation patterns and recording the integrated response within S1, our results provide insight into the ways that LC cells influence endogenous neural circuits in a multidimensional manner.

Short-latency responses in LC-modulated S1 neurons developed over repeated trials with either tonic or phasic LC stimulation, and this enhancement was not sensitive to the timing of phasic LC activation before or after the sensory stimulus. This global influence of NE on short-latency sensory-evoked cortical responses aligns with previous findings using electrical LC stimulation or direct NE application (16, 18, 37, 38, 42). Our recordings were made in deep-layer neurons in S1, and enhancements in short-latency responses have previously been demonstrated in deep pyramidal neurons that are sensitive to NE modulation of upstates (25, 43). Such modulation is driven by α1-noradrenergic, and not β-noradrenergic, signaling (32).

In addition to regulating salience, attention, and decision making, this system influences cortical arousal, which, in turn, may affect cortical responses to stimuli (30). In our previous work, we found that prolonged selective activation of LC-NE neurons using designer receptor technology increased arousal and emergence from isoflurane anesthesia (23). In the current study, we exclusively used LC photoactivation frequencies that did not induce arousal, as demonstrated by a lack of change in low-frequency EEG power. In this way, we were able to extract an arousal-independent role for LC in influencing cortical sensory processing. Thus, these results demonstrate a segregation in attentional vs. arousal functions for LC-NE activity, and indicate that LC-facilitated sensory/attentional processing does not depend upon LC-NE–induced changes in arousal.

LC-Driven Salience Encoding Across Cortical Targets. Our results show an enhancement of salience-like long-latency signaling, which was most prominent in our newly discovered LC-gated S1 neurons. We further demonstrated that nontuned LC-gated neurons are broadly distributed, comprising ∼40% of neurons in S1, and have distinctive characteristics both within and outside of sensory encoding. First, these neurons exhibited sensory detection only after LC activation (i.e., gating). Second, gated neurons had significantly lower baseline firing than LC-modulated neurons. Third, these neurons uniquely displayed large long-latency responses to salient sensory stimuli within a single trial. Fourth, these long-latency responses were sensitive to temporally specific manipulations of LC input. NE has previously been posited to "gate" target neurons by reducing the stimulus threshold of S1 neurons (10). Our findings indicate that LC-gated cells may be a distinct cortical phenotype (44, 45) that plays a specific role in encoding intensity and/or saliency information in cortex, and are not simply high-stimulus-threshold neurons.

LC-gated neurons also coordinate temporally with long-latency phasic LC-generated ERPs, forming a foundation for linking single-cell sensory encoding to global brain dynamics. In addition to our evidence for LC-mediated changes in local encoding of intensity/salience in S1, phasic LC activation elicited a cortical salience window that included N100- and P300-like ERPs in PFC. These ERPs are important neural signatures of attentional gating and sensory information encoding (28, 46, 47). During the salience window identified by the mPFC ERP, we saw parallel enhancement of long-latency S1 responses, essentially tagging intensity-like properties to the sensory event. The tight temporal specificity of the LC-mediated gain increases in target neurons during the salience window provides a mechanism by which LC-gated neurons may selectively facilitate encoding of behaviorally salient stimuli (48). As proposed in the adaptive gain theory of LC function (5), phasic activity and the broad efferent projections of LC may employ such gain mechanisms to facilitate execution of decisions and behavioral responses across brain networks. Future studies are needed to determine whether the impact of phasic LC activity on LC-gated populations is regulated by NE directly or by peptide corelease from LC-NE neurons, which can occur during phasic bursting (49).

Phasic LC as a Driver of P300. Elucidation of the neuronal basis of P300 ERPs is translationally relevant, as the P300 is measured in a wide range of cognitive and clinical studies in humans (47). Lesions to LC or its ascending fibers in the dorsal noradrenergic bundle diminish cortical P300 activity in both rodents and primates, which led to the proposal that LC is an important P300 mediator (28, 46, 50). Despite linking LC to P300 events, such lesion studies are limited by lack of specificity of lesion manipulations and potential compensatory responses after lesions. No prior studies demonstrated a neural circuit sufficient for de novo generation of cortical P300 signals, nor did they show the

relationship between neuronal dynamics in a defined circuit and P300. Our results provide causal evidence for phasic LC activity as a P300 generator, thereby defining a mechanism to support previous studies associating LC activity with P300 potentials. Our results show that phasic LC-evoked ERPs (including the P300 component) occur during encoding of salient sensory information, forming a translational biomarker of phasic LC activity.

Translational Implications. LC gating of cortical salience and intensity may be disrupted in a number of psychiatric and neurological conditions. Faulty regulation of salience signaling through LC dysfunction may underlie conditions characterized by persistent sensory hypersensitivity, including autism spectrum disorders and hyperalgesia (5, 51). Similarly, excessive attention devoted to irrelevant stimuli, as seen in attention deficit hyperactivity disorder, could be contributed to by LC-mediated "false salience." Based on the current results, such sensory hypersensitivity could be induced by a change in the prevalence or distribution of gated sensory neurons in primary cortical processing regions or by reduced thresholds for phasic LC activity, although future studies in disease models will be needed to clarify these mechanisms. Furthermore, these findings predict that disorders in which LC-NE neurons are damaged or lost, such as Alzheimer's disease or Parkinson's disease, could result in impairment of sensory information processing and attentional gating, which are well-established deficits with such disorders (52). Emphasizing the translational relevance of the current results, phasic LC-evoked ERP signals, as described here, could be used to investigate symptoms associated with LC dysregulation in such disorders while simultaneously providing a platform for cellular and molecular work in animal models to test potential therapeutic strategies.

Conclusions

Together, our results lead us to propose that a prominent role of sensory-locked phasic LC activity is to regulate sensory encoding and facilitate discrete saliency signals in cortical targets. Our evidence provides a mechanism for LC-facilitated enhancement of sensory attention that may underlie the role of LC in sensory-guided decisions. The phasic LC-driven changes in evoked cortical signaling exemplify the proposed adaptive gain mechanism of LC function (5). Thus, as predicted by adaptive gain theory, phasic LC activation, through broadly distributed, long-latency signaling, may facilitate context-dependent behavioral responses, including alerting and orienting toward an external signal or executing behavioral actions once an internal decision threshold has been reached. Both the P300 ERP and phasic LC activity have been strongly associated with decision making (5, 46), and our results identify a means by which salient stimuli may broadly influence cortical circuits through phasic LC activity to engage and optimize decision making and action execution.

Materials and Methods

Experimental Model and Subject Details. Twenty-one adult male Long–Evans rats (weighing >300 g at time of viral vector injection; Charles River Laboratories) were used for this study. Rats were housed in temperature- and humidity-controlled conditions, with ad libitum access to food and water in a 12-h light/dark cycle (06:00 lights off). All experimental procedures were undertaken during the animals' active diurnal cycle. All efforts were made to minimize the number of animals used and their suffering. All procedures strictly complied with Medical University of South Carolina Institutional Animal Care and Use Committee protocols and were in accordance with the guidelines described in the US NIH *Guide for the Care and Use of Laboratory Animals* (53).

Viral Vectors. Viral vectors were custom-packaged by the University of Pennsylvania viral vector core in vesicular stomatitis virus G protein pseudotyped lentiviral vectors. The synthetic PRSx8 promoter (22) was used to restrict expression of ChR2-mCherry to noradrenergic neurons after microinjection into LC (23, 24). Single-use aliquots of virus were prepared in a class II biosafety hood and stored at −80 °C until surgery.

Surgery. All surgeries were performed under isoflurane anesthesia. Viral vectors were delivered to LC from a glass pipette (35- to 40-μm tip) at anteroposterior (AP) − 3.8 (behind lambda), mediolateral (ML) ± 1.3, and 6.5–7.0 dorsoventral (nose tilted down 15°). One microliter of virus per side was delivered via brief pneumatic pulses (Picospritzer III; Parker Instruments) over ∼5 min. Animals were given at least 1 wk of recovery time before electrophysiology studies.

Electrophysiology.

LC recordings. For LC single-unit physiology, glass recording pipettes (5–12 MΩ) were filled with 2% Pontamine sky blue in 0.5 M sodium acetate. To record optogenetically evoked LC unit activity, the recording pipette was glued to a 200-μm-diameter optic fiber recessed 300 μm behind the recording tip. After craniotomy and dura retraction, the pipette was lowered until dorsal to LC coordinates to begin recording. Units were identified by standard criteria, including their characteristic wide action potentials, monophasic features in the unfiltered waveform, tonic baseline discharge rate of ∼1.5 Hz, phasic burst inhibition response to hind-paw pinch, and location relative to adjacent structures such as the mesencephalic trigeminal nucleus. LC units were amplified and filtered (300–3,000 Hz) through a Digitimer Neurolog system before digital conversion and recording to a microcomputer disk with Spike 2 (v5.21) via a Micro 1401 MkII interface (CED).

S1 recordings. LFPs (bandpass-filtered at 0.1–100 Hz) and single-neuron impulses (bandpass filtered at 100 Hz–8 kHz) were recorded from deep layers (V and VI) of the contralateral hind-limb region of S1 using 25-μm insulated stainless-steel wires in a 16-channel array through a Plexon MAP/16 recording system. Units were amplified, filtered, and sampled at 40 kHz before collection by RASPUTIN software (Plexon). During S1 recording, LC-NE neurons were photoactivated by 10-ms pulses of 473-nm light from a 200-μm-diameter optic fiber terminating 100–250 μm above the dorsal tip of LC; light pulses were delivered either tonically (3 Hz) or phasically (three pulses with 73-ms interpulse intervals, beginning 20 ms after paw stimulus).

EEG recordings. Bipolar twisted surface (–) to depth (+) electrodes (250-μm-diameter stainless steel) provided ipsilateral PFC EEG (bregma + 3.0 AP, ±1.0 ML) during LC and S1 recording. EEG signals were recorded differentially, filtered (0.1–50 Hz) through BMA-831/C amplifiers (CWE), and digitized at 1,000 Hz through CED Spike 2. Two superficial 30-gauge needles in the medial hind paw were used for sensory stimulation (0.5-ms pulse duration, 1-mA low-intensity pulse, 3-mA high-intensity pulse; AMPI ISO-Flex constant current stimulus isolation unit). Throughout all recordings, body temperature was monitored via rectal probe and maintained (36.0–37.5 °C) with an FHC thermistor-controlled heating pad.

Histology. After completion of experiments, animals were deeply anesthetized with 5% isoflurane and transcardially perfused with 0.9% saline and 4% paraformaldehyde before the brains were extracted. Tissue was postfixed overnight before cryoprotection in 20% PBS-sucrose azide. Four serial sets of 40-μm-thick coronal sections were collected on a cryostat (Leica) from the LC region and stored in PBS-sucrose azide at 4 °C until processing (160 μm between sections in each series). Transgene expression in LC was verified in all animals by processing with fluorescent double-label immunohistochemistry. Sections were rinsed three times for 5 min in PBS, followed by 1 h of blocking in PBS 0.1% Triton (PBST) with 3% normal donkey serum (immunobuffer). All antibodies were diluted in Immunobuffer, and tissue underwent parallel incubation with mouse anti-tyrosine hydroxylase (TH; 1:1,000; Immunostar) and rabbit anti-DsRed (1:500; Clontech) overnight. After three 5-min rinses in PBST, sections were incubated in donkey anti-mouse Alexa Fluor 488-conjugated (Invitrogen) and donkey anti-rabbit Alexa Fluor 594-conjugated (Invitrogen) secondary antibodies (1:500) for 3 h. For chromagen reaction of LC-ChR2 terminals in cortex, after incubation in DsRed primary antibody, tissue was incubated with donkey anti-rabbit SP biotin-conjugated secondary antibody (1:500; Jackson ImmunoResearch) for 2 h, followed by peroxidase substrate conjugation using an ABC Kit (Vector Laboratories). The mCherry staining was visualized with 3,3′-diaminobenzidine. All immunohistochemistry incubations were undertaken at room temperature on an orbital shaker. Tissue was rinsed in PBST before mounting in 0.1 M phostphate buffer and coverslipping with Citifluor AF1 antifade medium for fluorescence or with DPX (distyrene, plasticizer, and xylene) mounting medium for chromagen-stained tissue. All sections for analysis and presentation were imaged on a confocal laser-scanning microscope (Leica TCS SP5)

equipped with argon, argon/krypton, and helium/neon lasers. Channels were captured serially to avoid cross-excitation and bleedthrough.

Quantification and Statistical Analysis. Recording sites, optic fiber placements, and vector expression were positively verified histologically for all subjects included in the current study. Subjects not meeting appropriate placement and expression criteria (>60% LC coverage) were not used in any analyses. LC unit signals were sorted and analyzed using Spike 2 (v5.21). Phasic responses in LC units were computed using peri-event histograms from 50 trials of laser or 10-mA hind-paw stimulation. Response magnitudes in LC (RMag = count − baseline/trials) excitation was calculated during a 40-ms epoch poststimulation (0–40 ms laser, 20–60 ms after hind-paw stimulation) and normalized to 40 ms preceding the stimulus.

S1 units were sorted by template matching and principle component analysis in Offline Sorter (Plexon) and processed using custom MATLAB (MathWorks) scripts. Only well-isolated single units that fired throughout the entire duration of the recording session and that exhibited short-latency excitation (<50 ms) after 1-mA stimulation of the hind paw in at least one experimental condition (no laser, tonic or phasic stimulation) were included in analysis. All S1 unit activity was normalized to 500 ms of presensory stimulus baseline activity in the no-laser condition, and single-unit activity was binned with 1-ms resolution for short-latency responses (0–50 ms after sensory stimulus) or 10-ms resolution for long-latency responses (130–350 ms after sensory stimulus). Excitation was defined as one or more bins with $Z > 1.96$ (2 SD). S1 units were classified as LC-gated if short-latency responses were only seen with LC photoactivation and as LC-modulated if they demonstrated short-latency responses at baseline. EEG epochs and spectral densities were analyzed with NeuroExplorer (Nex Technologies) and custom MATLAB scripts. EEG δ and θ frequency bands were used for arousal measures based on previous literature of arousal-related frequencies under anesthesia (23, 54). ERP responses were averaged to the 500-ms prestimulus baseline voltage and averaged across 50 (phasic and tonic) or 300 (tonic) trials locked to LC laser pulses.

Parametric or nonparametric statistics, AUC calculations, and graph composition were undertaken in MATLAB and/or GraphPad Prism version 6.00 for Windows (GraphPad Software). $P < 0.05$ was the acceptable α level for all analyses. Colocalization of mCherry with TH was quantified with ImageJ (NIH). Any histological images were minimally processed for image-wide brightness and/or contrast, and all figures were compiled in Adobe Illustrator CS6.

ACKNOWLEDGMENTS. We thank Patrice Guyenet and Ruth Stornetta for original DNA constructs. Research was supported by Public Health Service Grants MH104716 (to E.M.V.) and MH092868 (to G.A.-J.).

1. Agster KL, Mejias-Aponte CA, Clark BD, Waterhouse BD (2013) Evidence for a regional specificity in the density and distribution of noradrenergic varicosities in rat cortex. *J Comp Neurol* 521:2195–2207.
2. Aston-Jones G, Shipley MT, Grazanna R (1995) The locus coeruleus, A5 and A7 noradrenergic cell groups. *The Rat Nervous System*, ed Paxinos G (Academic, New York), 2nd Ed, pp 183–214.
3. Clayton EC, Rajkowski J, Cohen JD, Aston-Jones G (2004) Phasic activation of monkey locus ceruleus neurons by simple decisions in a forced-choice task. *J Neurosci* 24: 9914–9920.
4. Aston-Jones G, Bloom FE (1981) Norepinephrine-containing locus coeruleus neurons in behaving rats exhibit pronounced responses to non-noxious environmental stimuli. *J Neurosci* 1:887–900.
5. Aston-Jones G, Cohen JD (2005) An integrative theory of locus coeruleus-norepinephrine function: Adaptive gain and optimal performance. *Annu Rev Neurosci* 28:403–450.
6. Berridge CW, Waterhouse BD (2003) The locus coeruleus-noradrenergic system: Modulation of behavioral state and state-dependent cognitive processes. *Brain Res Brain Res Rev* 42:33–84.
7. Bouret S, Sara SJ (2005) Network reset: A simplified overarching theory of locus coeruleus noradrenaline function. *Trends Neurosci* 28:574–582.
8. Bouret S, Sara SJ (2004) Reward expectation, orientation of attention and locus coeruleus-medial frontal cortex interplay during learning. *Eur J Neurosci* 20:791–802.
9. Armstrong-James M, Fox K (1983) Effects of ionophoresed noradrenaline on the spontaneous activity of neurones in rat primary somatosensory cortex. *J Physiol* 335: 427–447.
10. Waterhouse BD, et al. (1988) New evidence for a gating action of norepinephrine in central neuronal circuits of mammalian brain. *Brain Res Bull* 21:425–432.
11. Waterhouse BD, Woodward DJ (1980) Interaction of norepinephrine with cerebrocortical activity evoked by stimulation of somatosensory afferent pathways in the rat. *Exp Neurol* 67:11–34.
12. Adler LE, Pang K, Gerhardt G, Rose GM (1988) Modulation of the gating of auditory evoked potentials by norepinephrine: Pharmacological evidence obtained using a selective neurotoxin. *Biol Psychiatry* 24:179–190.
13. Rogawski MA, Aghajanian GK (1980) Norepinephrine and serotonin: Opposite effects on the activity of lateral geniculate neurons evoked by optic pathway stimulation. *Exp Neurol* 69:678–694.
14. Manella LC, Petersen N, Linster C (2017) Stimulation of the locus ceruleus modulates signal-to-noise ratio in the olfactory bulb. *J Neurosci* 37:11605–11615.
15. Devilbiss DM, Waterhouse BD (2000) Norepinephrine exhibits two distinct profiles of action on sensory cortical neuron responses to excitatory synaptic stimuli. *Synapse* 37: 273–282.
16. Bouret S, Sara SJ (2002) Locus coeruleus activation modulates firing rate and temporal organization of odour-induced single-cell responses in rat piriform cortex. *Eur J Neurosci* 16:2371–2382.
17. Waterhouse BD, Mouradian R, Sessler FM, Lin RC (2000) Differential modulatory effects of norepinephrine on synaptically driven responses of layer V barrel field cortical neurons. *Brain Res* 868:39–47.
18. Devilbiss DM, Waterhouse BD (2011) Phasic and tonic patterns of locus coeruleus output differentially modulate sensory network function in the awake rat. *J Neurophysiol* 105:69–87.
19. Abercrombie ED, Jacobs BL (1987) Single-unit response of noradrenergic neurons in the locus coeruleus of freely moving cats. I. Acutely presented stressful and non-stressful stimuli. *J Neurosci* 7:2837–2843.
20. Aston-Jones G, Rajkowski J, Kubiak P, Alexinsky T (1994) Locus coeruleus neurons in monkey are selectively activated by attended cues in a vigilance task. *J Neurosci* 14: 4467–4480.
21. Foote SL, Aston-Jones G, Bloom FE (1980) Impulse activity of locus coeruleus neurons in awake rats and monkeys is a function of sensory stimulation and arousal. *Proc Natl Acad Sci USA* 77:3033–3037.
22. Hwang DY, Carlezon WA, Jr, Isacson O, Kim KS (2001) A high-efficiency synthetic promoter that drives transgene expression selectively in noradrenergic neurons. *Hum Gene Ther* 12:1731–1740.
23. Vazey EM, Aston-Jones G (2014) Designer receptor manipulations reveal a role of the locus coeruleus noradrenergic system in isoflurane general anesthesia. *Proc Natl Acad Sci USA* 111:3859–3864.
24. Abbott SB, et al. (2009) Photostimulation of retrotrapezoid nucleus phox2b-expressing neurons in vivo produces long-lasting activation of breathing in rats. *J Neurosci* 29:5806–5819.
25. Constantinople CM, Bruno RM (2011) Effects and mechanisms of wakefulness on local cortical networks. *Neuron* 69:1061–1068.
26. Carter ME, et al. (2010) Tuning arousal with optogenetic modulation of locus coeruleus neurons. *Nat Neurosci* 13:1526–1533.
27. Usher M, Cohen JD, Servan-Schreiber D, Rajkowski J, Aston-Jones G (1999) The role of locus coeruleus in the regulation of cognitive performance. *Science* 283:549–554.
28. Ehlers CL, Chaplin RI (1992) Long latency event related potentials in rats: The effects of changes in stimulus parameters and neurochemical lesions. *J Neural Transm (Vienna)* 88:61–75.
29. Parasuraman R, Beatty J (1980) Brain events underlying detection and recognition of weak sensory signals. *Science* 210:80–83.
30. Chapin JK, Waterhouse BD, Woodward DJ (1981) Differences in cutaneous sensory response properties of single somatosensory cortical neurons in awake and halothane anesthetized rats. *Brain Res Bull* 6:63–70.
31. Mountcastle VB (1957) Modality and topographic properties of single neurons of cat's somatic sensory cortex. *J Neurophysiol* 20:408–434.
32. Mouradian RD, Sessler FM, Waterhouse BD (1991) Noradrenergic potentiation of excitatory transmitter action in cerebrocortical slices: Evidence for mediation by an alpha 1 receptor-linked second messenger pathway. *Brain Res* 546:83–95.
33. Bekavac I, Waterhouse BD (1995) Systemically administered cocaine selectively enhances long-latency responses of rat barrel field cortical neurons to vibrissae stimulation. *J Pharmacol Exp Ther* 272:333–342.
34. Aston-Jones G, Foote SL, Bloom FE (1982) Low doses of ethanol disrupt sensory responses of brain noradrenergic neurones. *Nature* 296:857–860.
35. Sara SJ, Bouret S (2012) Orienting and reorienting: The locus coeruleus mediates cognition through arousal. *Neuron* 76:130–141.
36. Dayan P, Yu AJ (2006) Phasic norepinephrine: A neural interrupt signal for unexpected events. *Network* 17:335–350.
37. Woodward DJ, Moises HC, Waterhouse BD, Hoffer BJ, Freedman R (1979) Modulatory actions of norepinephrine in the central nervous system. *Fed Proc* 38:2109–2116.
38. Sessler FM, et al. (1995) Noradrenergic enhancement of GABA-induced input resistance changes in layer V regular spiking pyramidal neurons of rat somatosensory cortex. *Brain Res* 675:171–182.
39. Bevan P, Bradshaw CM, Roberts MH, Szabadi E (1973) The excitation of neurons by noradrenaline. *J Pharm Pharmacol* 25:309–314.
40. Waterhouse BD, Moises HC, Woodward DJ (1980) Noradrenergic modulation of somatosensory cortical neuronal responses to iontophoretically applied putative neurotransmitters. *Exp Neurol* 69:30–49.
41. Foote SL, Freedman R, Oliver AP (1975) Effects of putative neurotransmitters on neuronal activity in monkey auditory cortex. *Brain Res* 86:229–242.
42. Ikeda MZ, Jeon SD, Cowell RA, Remage-Healey L (2015) Norepinephrine modulates coding of complex vocalizations in the songbird auditory cortex independent of local neuroestrogen synthesis. *J Neurosci* 35:9356–9368.
43. Safaai H, Neves R, Eschenko O, Logothetis NK, Panzeri S (2015) Modeling the effect of locus coeruleus firing on cortical state dynamics and single-trial sensory processing. *Proc Natl Acad Sci USA* 112:12834–12839.

44. Vijayan S, Hale GJ, Moore CI, Brown EN, Wilson M (2010) Activity in the barrel cortex during active behavior and sleep. *J Neurophysiol* 103:2074–2084.
45. McCormick DA, Connors BW, Lighthall JW, Prince DA (1985) Comparative electrophysiology of pyramidal and sparsely spiny stellate neurons of the neocortex. *J Neurophysiol* 54:782–806.
46. Nieuwenhuis S, Aston-Jones G, Cohen JD (2005) Decision making, the P3, and the locus coeruleus-norepinephrine system. *Psychol Bull* 131:510–532.
47. Polich J (2007) Updating P300: An integrative theory of P3a and P3b. *Clin Neurophysiol* 118: 2128–2148.
48. Servan-Schreiber D, Printz H, Cohen JD (1990) A network model of catecholamine effects: Gain, signal-to-noise ratio, and behavior. *Science* 249:892–895.
49. Holets VR, Hökfelt T, Rökaeus A, Terenius L, Goldstein M (1988) Locus coeruleus neurons in the rat containing neuropeptide Y, tyrosine hydroxylase or galanin and their efferent projections to the spinal cord, cerebral cortex and hypothalamus. *Neuroscience* 24:893–906.
50. Pineda JA, Foote SL, Neville HJ (1989) Effects of locus coeruleus lesions on auditory, long-latency, event-related potentials in monkey. *J Neurosci* 9:81–93.
51. Gonzalez-Gadea ML, et al. (2015) Predictive coding in autism spectrum disorder and attention deficit hyperactivity disorder. *J Neurophysiol* 114:2625–2636.
52. Conte A, Khan N, Defazio G, Rothwell JC, Berardelli A (2013) Pathophysiology of somatosensory abnormalities in Parkinson disease. *Nat Rev Neurol* 9:687–697.
53. National Research Council (2011) *Guide for the Care and Use of Laboratory Animals* (National Academies Press, Washington, DC), 8th Ed.
54. Berridge CW, Foote SL (1991) Effects of locus coeruleus activation on electroencephalographic activity in neocortex and hippocampus. *J Neurosci* 11: 3135–3145.